Contribution to Stability and Folding of a Buried Polar Residue at the CARM1 Methylation Site of the KIX Domain of CBP†

Yu Wei,‡ Jia-Cherng Horng,§ Andrew C. Vendel,‡ Daniel P. Raleigh,§,|| and Kevin J. Lumb*,‡,⊥

Department of Biochemistry and Molecular Biology and Department of Chemistry, Colorado State University, Fort Collins, Colorado 80523-1870, and Department of Chemistry, Graduate Program in Biophysics, and Graduate Program in Biochemistry and Structural Biology, State University of New York, Stony Brook, New York 11794-3400

Received March 12, 2003

ABSTRACT: The transcriptional coactivator and acetyltransferase CREB Binding Protein (CBP) is comprised of several autonomously folded and functionally independent domains. The KIX domain mediates interactions between CBP and numerous transcriptional activators. The folded region of KIX has all the structural features of a globular protein, including three α-helices, two short 3_{10} helices, and a well-packed hydrophobic core. KIX contains a buried cation−π interaction between the positively charged guanidinium group of Arg 600 and the aromatic ring of Tyr 640. Arg 600 is a site for regulatory methylation by CARM1/PRMT4, which negates the CREB-binding function of the KIX domain. The role of the Arg 600−Tyr 640 buried polar interaction in specifying and stabilizing the structure of KIX was investigated by comparing the folding of wild-type KIX with the single point mutants Y640F and R600M. The Y640F mutant disrupts a hydrogen bond involving the Tyr 640 OH and the backbone of V595 but still allows for the cation−π interaction while the R600M mutant disrupts the cation−π interaction. Both wild type KIX and Y640F exhibit properties expected of native like, globular proteins such as a single oligomerization state (monomer), cooperative thermal and urea-induced unfolding transitions, and a well-packed core. In contrast, the R600M mutant has properties reminiscent of a molten globule state, including a tendency to aggregate, noncooperative thermal unfolding transition, and a loosely packed core. Thus, the buried cation−π interaction is critical for specifying the unique cooperatively folded structure of KIX.

Structural uniqueness is a remarkable property of globular proteins. Naturally occurring proteins typically populate an ensemble of closely related conformations with many efficiently packed side chains in a hydrophobic core that excludes solvent. Buried polar interactions of appropriate geometry provide one effective mechanism to impart structural uniqueness (*1*, *2*). Buried hydrogen bonds or salt bridges involving side chains are a common feature of natural proteins (*3*, *4*) and have been shown in numerous cases to impart nativelike properties and levels of structural uniqueness in coiled coils, helical bundles, and globular proteins (*1*, *2*, *5*−*11*). In addition to conventional hydrogen bonds and salt bridges, cation−π interactions involving positively charged Lys or Arg side chains and aromatic rings also provide a source of buried polar interactions. The cation−π interaction is a common feature of proteins that occurs about once every 77 residues, or about half as frequently as salt bridges (*12*). The interaction has received attention in terms of ligand binding and protein stability (*12*, *13*).

The transcriptional coactivator and acetyltransferase CBP[1] and the highly related but distinct p300 contribute to the regulation of gene expression in processes such as cell growth, differentiation, and tumor suppression (*14*, *15*). Human CBP is a large protein (2441 amino acids) that is comprised of several autonomously folded and functionally independent domains (*14*, *15*). One domain, called KIX, mediates interactions between CBP and numerous mammalian and viral transcriptional activators such as CREB, p53, and HIV-1 Tat (*14*−*16*). The human and mouse KIX domains of CBP and p300 share 100% sequence identity over the folded region of KIX (residues 587−667 of human CBP). The folded region of KIX has all the structural features of a globular protein (*17*). KIX contains three α-helices, two short 3_{10} helices, and interconnecting loops that form a globular fold around a hydrophobic core (Figure 1).

KIX contains a buried cation−π interaction between the positively charged guanidinium group of Arg 600 and the aromatic ring of Tyr 640 in the NMR structure of the KIX

† Supported by NIH grant R01 GM54233 (DPR) and American Cancer Society grant RSG-02-051-GMC (KJL).

* Corresponding author. E-mail: lumb@lamar.colostate.edu.

‡ Department of Biochemistry and Molecular Biology, Colorado State University.

§ Department of Chemistry, State University of New York.

|| Graduate Program in Biophysics and Graduate Program in Biochemistry and Structural Biology, State University of New York.

⊥ Department of Chemistry, Colorado State University.

[1] Abbreviations: [θ], molar ellipticity; $[\theta]_{222}$, molar ellipticity at 222 nm; $\Delta G_u°$, free energy of unfolding; ANS, 1-anilinonaphthalene 8-sulfonate; CARM1, coactivator-associated arginine methyltransferase 1; CBP, CREB-binding protein; C_m, midpoint of the denaturant-induced unfolding transition; CREB, cyclic AMP response element binding protein; CD, circular dichroism; HPLC, high-performance liquid chromatography; LB, Luria−Bertani; NMR, nuclear magnetic resonance; PCR, polymerase chain reaction; PRMT4, protein arginine *N*-methyltransferase 4; T_m, midpoint of the thermal unfolding transition.

10.1021/bi0343976 CCC: $25.00
Published on Web 05/23/2003

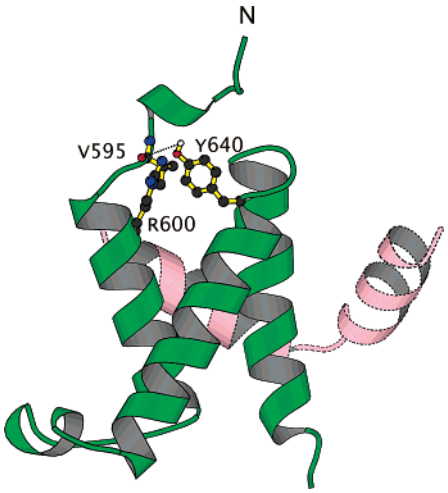

FIGURE 1: Structure of the KIX domain (green) bound to the KID region of CREB (pink). Arg 600, Tyr 640, and Val 595 are on the opposite side of KIX to the KID binding site. The Arg 600 side chain is approximately 75% buried, with an average solvent accessibility (1.4 Å probe) of 52 Å^2, and a range of 34−72 Å^2, over the 17 members of the NMR structure family. The Tyr 640 side chain is essentially fully buried, with an average solvent accessibility of 7 Å^2 and a range of 0−22 Å^2. The average distance in the 17 NMR structures from the Arg 600 guandinium group carbon to the center of the Try 640 ring is 4.5 Å. The range is 3.4−6.0 Å and for 12 of the 17 structures the distance is less than 5 Å.

domain of CBP bound to the KID region of CREB (*17*).[2] Arg 600 and Tyr 640 are conserved in the KIX domains of mouse and human CBP and p300, as are the other residues that comprise the folded region of KIX (*17*). Tyr 640 of CBP also forms a buried hydrogen bond with Val 595 CO (*17*). The buried polar cation−π interaction and hydrogen bond involving Tyr 640 have the potential to contribute to the protein-folding specificity and stability of KIX.

Arg 600 of p300 is a site for posttranslational methylation by CARM1/PRMT4 (*18*). CARM1 is a type I arginine methyltransferase that catalyzes formation of ω-N^G-monomethyl arginine and asymmetric ω-N^G,N^G-dimethylarginine (*19*, *20*). In vitro, CARM1 methylates the RNA-binding protein HuR, histone H3, and p300/CBP (*18*−*22*). Methylation of Arg 600 of the KIX domain by CARM1 negatively regulates the ability of KIX to bind CREB and interferes with CREB-mediated pathways (*18*). Arg 600 is remote from the CREB binding site of KIX (Figure 1), and so it is unlikely that Arg 600 methylation introduces a direct steric impediment to CREB binding. Methylation might, however, modulate the cation−π interaction between Arg-600 and Tyr-640.

Here we characterize the folding properties of KIX mutants in which the Arg 600-Tyr 640 interaction is probed with the conservative mutations R600M and Y640F. The wild-type and Y640F mutant adopt stable structures with the properties expected of a well-folded, nativelike globular protein. In contrast, the single substitution of Arg 600 with Met results in a helical structure with properties reminiscent of the molten globule. Our results suggest that the neutralization of Arg 600 by mutagenesis and loss of the R600−Y640 buried polar cation−π interaction arrests folding at a molten globule-like state and prevents folding to the well-defined structure typical of a folded, globular protein.

[2] While the human KIX domain is used here, the mouse CBP sequence numbering is used for ease of comparison with the majority of studies that use mouse CBP.

MATERIALS AND METHODS

KIX Expression and Purification. KIX, corresponding to residues 588−679 of human CBP with an additional N-terminal Met, was expressed in *Escherichia coli* strain BL21 (DE3) pLysS and purified as described previously (*23*, *24*). Final purification was by reversed-phase C18 HPLC. The identity and integrity of KIX was confirmed with electrospray mass spectrometry, and for all preparations the expected and observed mass agreed to within 1 Da.

KIX Mutagenesis. Expression plasmids for the KIX mutants R600M and Y640F were prepared by site-directed mutagenesis of pET3a-KIX (23) using the Quikchange PCR protocol (Stratagene). Plasmids were sequenced with dRhodamine automated sequencing.

Expression and Purification of Y640F. Y640F was expressed and purified in the same way as wild-type KIX (*23*, *24*). The identity of each Y640F preparation was confirmed with electrospray mass spectrometry, and in all cases the expected and observed mass agreed to within 1 Da.

Expression and Purification of R600M. R600M was expressed in *E. coli* strain BL21 (DE3) pLysS. The yield of R600M was much less than that of KIX, and a different purification strategy was required. Cells were grown until the optical density at 600 nm was 1, induced with 1 mM IPTG for 3 h, harvested by centrifugation, resuspended in 10 mM Tris-base, 1 mM EDTA, pH 7.5, and lysed by sonication. R600M was purified from soluble fraction with HiTrap Q and SP columns (Pharmacia) equilibrated in 10 mM Tris, 1 mM EDTA, pH 7.5. R600M was present in the Q and SP flow throughs. Final purification was by reversed-phase C18 HPLC. The final yield of R600M from LB medium was approximately 25 μg/L. The identity of R600M was confirmed with MALDI mass spectrometry and the observed and expected mass agreed to within 1 Da.

Protein Concentration Determination. The concentrations of protein stock solutions were determined by Tyr absorbance in 6 M GuHCl, 10 mM sodium phosphate, and 50 mM NaCl, pH 6.5 at 25 °C, using an extinction coefficient at 276 nm of 12 650 cm^{-1} M^{-1} for KIX and R600M, and 11 200 cm^{-1} M^{-1} for Y640F (*25*).

Circular Dichroism Spectroscopy. CD spectroscopy was performed with an Aviv 202 spectrometer. Samples contained 10 μM protein in 10 mM sodium phosphate and 150 mM NaCl, pH 6.0.

Thermal stability was monitored from the change in $[\theta]_{222}$ with temperature. The T_m was estimated from the first derivative of the change in $[\theta]_{222}$ with respect to $1/T$ as T was changed in 1 K steps (*26*).

Chemical denaturation was monitored at 25 °C from the change in $[\theta]_{222}$ upon titration with urea. Urea concentration was determined with refractometry (*27*). The free energy of unfolding ($\Delta G_u°$) and m were obtained with nonlinear least-squares fitting of the unfolding curve assuming a monomer unfolding model (*28*, *29*).

Fluorescence Spectroscopy. Fluorescence studies of urea denaturation were performed with a Spex ISA Fluorolog spectrometer. Chemical-denaturation data was monitored at 25 °C from the change in emission intensity at 355 nm using

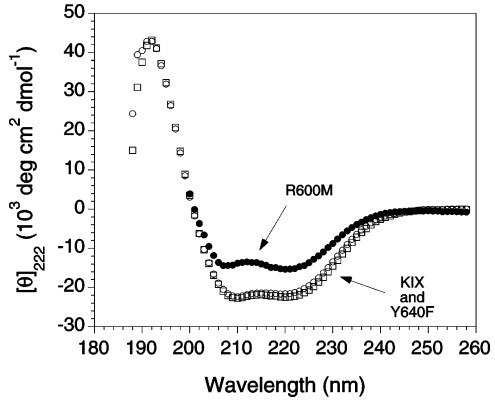

FIGURE 2: CD spectra of KIX (○), R600M (●), and Y640F (□) (10 μM protein concentration, 10 mM sodium phosphate, 150 mM NaCl, pH 6.0, 25 °C). The minima at 208 and 222 nm indicate that the proteins form helical structures.

an excitation wavelength of 276 nm upon titration with urea. Samples contained 5 μM protein in 10 mM sodium phosphate and 150 mM NaCl, pH 6.0. Urea concentration was determined with refractometry (*27*). The free energy of unfolding ($\Delta G_u°$) and *m* were obtained with nonlinear least-squares fitting of the unfolding curve to a monomer unfolding model (*28*, *29*).

Fluorescence studies of ANS binding were performed with an Aviv ATF-105 spectrometer. ANS binding was monitored at 25 °C using an excitation wavelength of 355 nm and an emission wavelength range of 400−600 nm. Samples contained 5 μM ANS (Molecular Probes) and 5−100 μM KIX, Y640F, or R600M at pH 6.0 or 5−100 μM bovine α-lactalbumin (Sigma) at pH 2. Samples were prepared in 10 mM sodium phosphate and 150 mM NaCl. ANS concentration was determined for a stock solution in methanol by absorbance at 372 nm using an extinction coefficient of 7.8×10^3 cm^{-1} M^{-1} (supplied by Molecular Probes).

Analytical Ultracentrifugation. Sedimentation equilibrium was performed with a Beckman XL-I analytical ultracentrifuge. Samples were dialyzed overnight against the reference buffer (10 mM sodium phosphate and 150 mM NaCl, pH 6.0). Data were collected at 35 and 45 krpm at 25 °C at 280 nm. Equilibrium was judged to be reached when three scans taken at 2 h intervals were essentially identical. A solvent density of 1.004 g ml^{-1} and a partial molar volume of 0.74 mL g^{-1} were used (*30*). Data were fit with ORIGIN 4.1 (Beckman Instruments) to an ideal, single-species model.

RESULTS

KIX Adopts a Monomeric, Nativelike Fold. The CD spectrum of KIX is characteristic of a highly helical protein (Figure 2), with minima at the helical signature wavelengths of 208 and 222 nm. This result is in accord with previous CD studies (*16*, *23*, *24*) and the NMR structure of KIX (*17*). Sedimentation equilibrium data for KIX are accounted for by a single-species monomer (Figure 3). The observed mass is 11.5 kDa ± 0.2 kDa, which is within error of the expected mass of 11 139.8 Da. The observed mass does not change systematically with KIX concentration or rotor speed (Table 1), suggesting that KIX behaves as an ideal, single species monomer.

The temperature-induced unfolding transition of KIX monitored with CD spectroscopy at 222 nm is sigmodial with

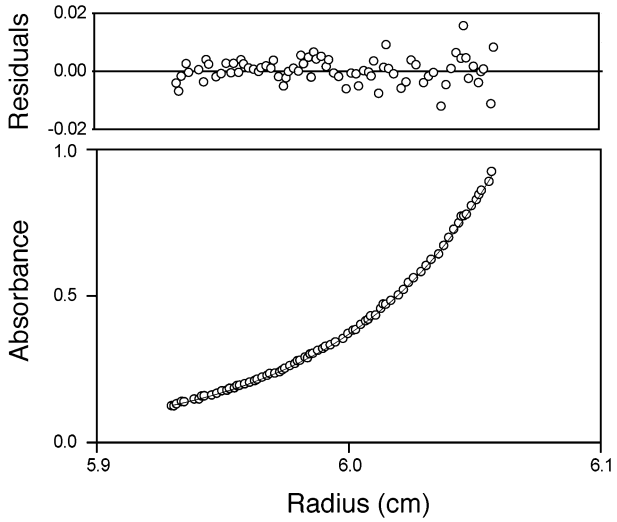

FIGURE 3: Sedimentation equilibrium indicates that KIX is monomeric (45 krpm, 30 μM total KIX concentration, 10 mM sodium phosphate, 150 mM NaCl, pH 6.0, 25 C). The data are accounted for with an ideal, single-species model, as shown by the random distribution of residuals.

Table 1: Sedimentation Equilibrium Data

total protein concentration	mass at specified rotor speed	
	35 krpm	45 krpm
KIX		
15 μM	11.65 kDa	11.11 kDa
43 μM	11.50 kDa	11.40 kDa
63 μM	11.47 kDa	11.63 kDa
Y640F		
30 μM	11.13 kDa	11.76 kDa
56 μM	10.86 kDa	11.92 kDa
80 μM	11.50 kDa	10.02 kDa
R600M		
22 μM	19.21 kDa	15.78 kDa
30 μM	19.85 kDa	18.21 kDa
39 μM	21.06 kDa	19.85 kDa

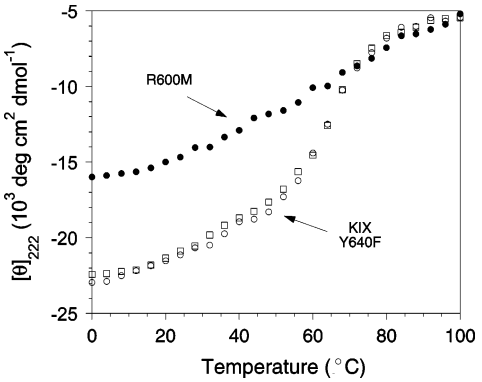

FIGURE 4: Thermal stability of KIX (○), R600M (●), and Y640F (□) monitored with the temperature dependence of $[\theta]_{222}$ (10 μM protein concentration, 10 mM sodium phosphate, 150 mM NaCl, pH 6.0, 25 °C). KIX and Y640F exhibit very similar sigmodial unfolding transitions of equivalent T_m (65 °C). R600M exhibits a linear thermal melt, which is reminiscent of the properties of the molten globule.

a T_m of 65 ± 2 °C (Figure 4). The thermal unfolding and folding curves are essentially superimposable (data not shown), showing that the thermal-unfolding transition is reversible. The urea-induced unfolding transition of KIX monitored with both CD at 222 nm and fluorescence

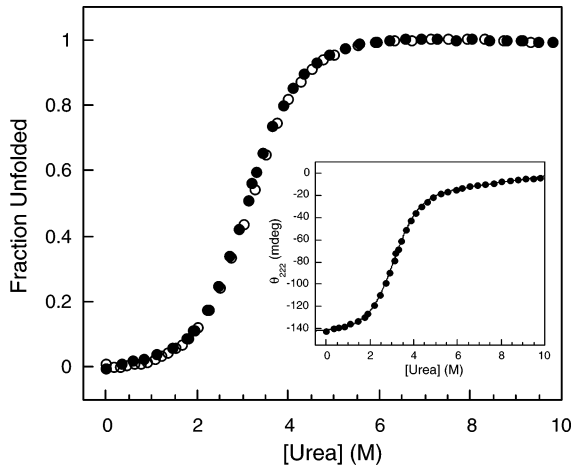

FIGURE 5: Urea-induced unfolding of KIX (●) and Y640F (○) monitored with CD at 222 nm (10 μM protein concentration, 10 mM sodium phosphate, 150 mM NaCl, pH 6.0, 25 °C). KIX and Y640F exhibit very similar sigmodial unfolding transitions of equivalent C_m (3.1 M).

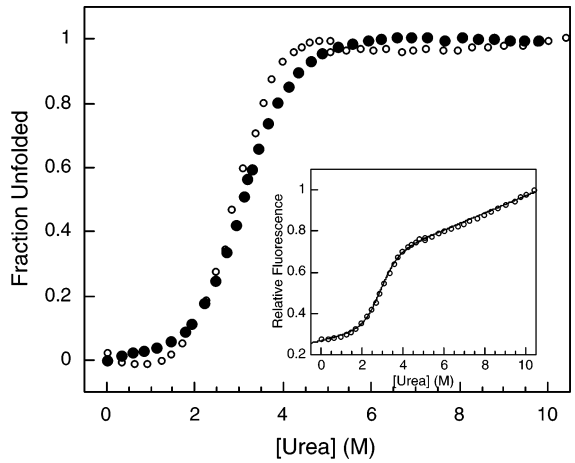

FIGURE 6: Evaluation of two-state unfolding of KIX as monitored with fluorescence (insert) and CD (Figure 5). The urea-induced unfolding transitions of KIX monitored with fluorescence (○) and CD (●) in terms of fraction unfolded are not equivalent, suggesting that unfolding may not be two state.

emission at 355 nm is also sigmoidal (Figures 5 and 6). Such behavior is typical for a nativelike globular protein. The sigmodial thermal and urea unfolding curves suggest that KIX is cooperatively folded, as expected for a nativelike globular protein.

The KIX unfolding curves monitored with CD and fluorescence in terms of fraction unfolded are not exactly equivalent, although the C_m values of 3.1 and 2.9 M determined with CD and fluorescence, respectively, are essentially identical (Figure 6). This observation suggests that unfolding may not be strictly two-state. The analysis of the fluorescence data is complicated by the significant slope of the posttransition baseline and the short pretransition baseline (Figure 6), and thus it is difficult to judge the significance of the apparent deviation from two-state behavior. The evaluation of the true thermodynamic stability of KIX awaits further detailed kinetic and equilibrium studies to determine the multistate nature of the unfolding transition. Analysis of the CD data assuming a two-state transition gives an apparent $\Delta G_u^\circ = 3.4 \pm 0.1$ kcal/mol and $m = 1.07$ kcal mol^{-1} mol^{-1} (measured at Colorado State University) or 3.3

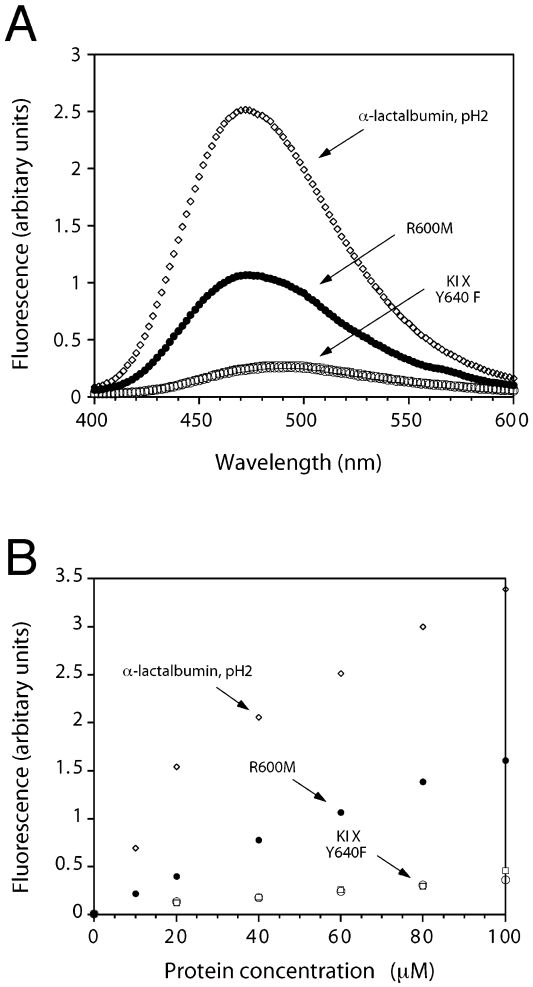

FIGURE 7: Fluorescence studies of ANS binding. (A) Emission scans of ANS (5 μM) in the presence of 60 μM protein. (B) Changes in emission intensity of ANS upon titration with protein. The pH 2 α-lactalbumin molten globule induces a significant increase in the emission intensity of ANS and a shift in emission wavelength maximum form 484 to 470 nm, in accord with previous results (*33*). KIX and Y640F do not induce significant changes in ANS fluorescence, indicating a lack of ANS binding and hence the presence of a well-packed interior. In contrast, R600M induces changes in ANS emission intensity and wavelength, suggesting the presence of a loosely packed core that sequesters ANS.

$\pm$ 0.1 kcal/mol and $m = 1.05$ kcal mol^{-1} mol^{-1} (measured at State University of New York) (Figure 5).

KIX does not bind ANS appreciably, as compared to the classic molten globule pH 2 form of α-lactalbumin (Figure 7). Folded, globular proteins typically bind ANS weakly, if at all, whereas molten globules and loosely packed proteins bind ANS avidly, presumably because these proteins do not possess a tightly packed hydrophobic core (*31*−*35*). The finding that KIX does not bind ANS suggests that KIX has a well-packed hydrophobic core that excludes solvent, as expected for a nativelike, globular protein.

The R600M Mutant Adopts a Molten Globule-Like Fold. The CD spectrum of R600M is characteristic of a helical protein, although the intensity of the signature bands for helix formation at 208 and 222 nm are reduced compared to wild-type KIX (Figure 2). The change in CD signal at 222 nm with temperature is linear, implying that R600M is not cooperatively folded (Figure 4). The R600M mutant is not monomeric, with an observed mass that increases systemati-

cally with total concentration and is intermediate between that expected of the monomer (11.1 kDa) and the dimer (22.2 kDa) (Table 1). These results indicate that R600M is aggregating. In addition, the R600M mutant binds ANS (Figure 7), implying the presence of a loosely packed interior. Further biophysical characterization is hindered by the low yield of R600M (approximately 25 μg per liter of culture). The properties of secondary structure formation, noncooperative thermal unfolding, aggregation, and ANS binding are reminiscent of the classic molten globule (*35*).

Benign Consequences of the Y640F Mutation. The aromatic ring of Y640 forms a cation$-\pi$ interaction with Arg 600, and Y640 OH forms a hydrogen bond with Val 595 CO (*17*). The Y640F mutation would be expected to disrupt the Tyr 640−Val 595 hydrogen bond, but not the Y640−R600 cation$-\pi$ interaction. Sedimentation equilibrium indicates that the Y640F mutant is monomeric. The mass expected for a monomer is 11 123.8 Da, and the observed mass is 11.4 ± 0.4 kDa (Table 1). The observed mass does not change systematically with protein concentration or rotor speed (Table 1). The CD spectra of the folded states of the wild-type and Y640F mutant are essentially identical (Figure 2). The thermal and urea-induced unfolding curves of KIX and Y640F are also similar, with the same apparent T_m and C_m values (Figures 4 and 5). Finally, Y640F does not bind ANS (Figure 7). These results indicate that the stability and structural properties of wild-type and Y640F KIX are essentially identical.

DISCUSSION

Elucidating the mechanisms of protein folding and the successful design of proteins with nativelike properties requires understanding the interactions within globular proteins that contribute to structural uniqueness. Buried polar interactions that destabilize alternative conformations that do not satisfy the ionic bonding potential of buried polar groups provide one route to impart structural uniqueness (*1*, *2*). Buried hydrogen bonds and salt bridges impart structural uniqueness in natural and designed coiled-coils, helical bundles, and the globular protein thioredoxin (*1*, *2*, *5*−*8*, *24*, *9*, *11*). Not all buried polar interactions, however, contribute to structural uniqueness, as seen for the Fyn and CrK SH3 domains and Arc repressor (*36*−*38*). In addition to buried hydrogen bonds and salt bridges, buried polar cation$-\pi$ interactions between aromatic groups and guandinium groups provide a potential mechanism to confer structural uniqueness. Cation$-\pi$ interactions are a common feature of protein structures and of protein−ligand interactions that occur about half as frequently as salt bridges (*12*, *13*).

The globular KIX domain of the transcriptional coactivator and acteyltransferase CBP contains a buried cation$-\pi$ interaction between the aromatic ring of Tyr 640 and the guandinium group of Arg 600 (*17*). KIX exhibits the hallmarks of a globular protein, including the signature biophysical properties of a discrete (monomeric) oligomerization state, sigmoidal temperature and denaturant-induced unfolding transitions, and a well-packed interior that excludes ANS.

Disruption of the buried cation$-\pi$ interaction by the replacement of Arg 600 with Met results in a protein with properties more closely aligned with those of the partially folded molten globule. Indeed, the tendency to aggregate, linear thermal melt, and poorly packed hydrophobic core, as suggested by the avidity for ANS, are all properties of the classic molten globule and designed proteins that lack structural uniqueness (*35*, *39*, *40*). The key role of Arg 600 in imparting structural uniqueness to KIX no doubt reflects the conservation of Arg 600 in KIX domains across species (*17*). This finding indicates that, in addition to buried salt bridges and side chain hydrogen bonds (*1*, *2*, *5*−*8*, *24*, *9*, *11*), buried polar cation$-\pi$ interactions can impart structural uniqueness to protein folding.

Y640 OH also forms a buried hydrogen bond with V595 CO (*17*). In contrast to the striking effects of the R600M mutation, the Y640F mutation does not result in any measurable changes in stability or folding. This finding is consistent with the aromatic ring forming a cation$-\pi$ interaction with the R600 side chain. It also suggests that the buried hydrogen bond involving Y640 OH and V595 CO makes a net minimal contribution to both structural uniqueness and stability. The observation that Y640 forms two buried polar interactions with very different consequences for KIX folding and stability highlights the role of context and degeneracy of polar interactions in imparting stability and specificity to protein structure.

Protein methylation has recently garnered attention as a mechanism of protein regulation (*41*, *42*). Arg 600 methylation by CARM1 negatively regulates the ability of KIX to bind CREB and of CBP to act as a coactivator (*18*). Since Arg 600 is distant to the CREB binding site (*17*), it is unlikely that the methylation of Arg 600 interferes directly with CREB binding. Arg 600 methylation may, however, disrupt the native folding properties of KIX in a way that is analogous to the R600M mutation. It is intriguing to speculate that posttranslational modifications may provide a cellular mechanism of protein regulation by the disruption of protein folding.

In conclusion, the cation$-\pi$ buried polar interaction involving Arg 600 and Tyr 640 plays a crucial role in imparting folding specificity to the KIX domain of CBP. The results emphasize the contribution of buried polar interactions to protein folding and specificity, and extend the repertoire of mechanisms available for the design of proteins with nativelike properties.

ACKNOWLEDGMENT

We thank K. M. Campbell for valuable discussions.

NOTE ADDED AFTER ASAP POSTING

This paper was posted inadvertently 05/23/03 and included two mentions of 3^{10} helices (one in the abstract and one in the second paragraph of the text) instead of 3_{10} helices. The correct version of this paper was posted 05/27/03.

REFERENCES

1. Lumb, K. J., and Kim, P. S. (1995) *Biochemistry 34*, 8642−8648.
2. Raleigh, D. P., Betz, S. F., and DeGrado, W. F. (1995) *J. Am. Chem. Soc.* 7558−7559.
3. Barlow, D. J., and Thornton, J. M. (1983) *J. Mol. Biol. 168*, 867−885.
4. Rashin, A. A., and Honig, B. (1984) *J. Mol. Biol. 173*, 515−521.
5. Schneider, J. P., Lear, J. D., and DeGrado, W. F. (1997) *J. Am. Chem. Soc. 119*, 5742−5743.

6. Oakley, M. G., and Kim, P. S. (1998) *Biochemistry 37*, 12603−12610.
7. Zhu, H., Celinski, S. A., Scholtz, J. M., and Hu, J. C. (2000) *J. Mol. Biol. 300*, 1377−1387.
8. Bolon, D. N., and Mayo, S. L. (2001) *Biochemistry 40*, 10047−10053.
9. Campbell, K. M., and Lumb, K. J. (2002) *Biochemistry 41*, 7169−7175.
10. Campbell, K. M., Sholders, A. J., and Lumb, K. J. (2002) *Biochemistry 41*, 4866−4871.
11. McClain, D. L., Gurnon, D. G., and Oakley, M. G. (2002) *J. Mol. Biol. 324*, 257−270.
12. Gallivan, J. P., and Dougherty, D. A. (1999) *Proc. Natl. Acad. Sci. U.S.A. 96*, 9459−9464.
13. Zacharias, N., and Dougherty, D. A. (2002) *Trends Pharm. Sci. 23*, 281−287.
14. Goodman, R. H., and Smolik, S. (2000) *Genes Dev. 14*, 1553−1577.
15. Chan, H. M., and La Thangue, N. B. (2001) *J. Cell Sci. 114*, 2363−2373.
16. Vendel, A. C., and Lumb, K. J. (2003) *Biochemistry 42*, 910−916.
17. Radhakrishnan, I., Pérez-Alvarado, G. C., Parker, D., Dyson, H. J., Montminy, M. R., and Wright, P. E. (1997) *Cell 91*, 741−752.
18. Xu, W., Chen, H., Du, K., Asahara, H., Tini, M., Emerson, B. M., Montminy, M., and Evans, R. M. (2001) *Science 294*, 2507−2511.
19. Chen, D., Ma, H., Hong, H., Koh, S. S., Huang, S., Schurter, B. T., Aswad, D. W., and Stallcup, M. R. (1999) *Science 284*, 2174−2177.
20. Schurter, B. T., Koh, S. S., Chen, D., Bunick, G. J., Harp, J. M., Hanson, B. L., Henschen-Edman, A., Mackay, D. R., Stallcup, M. R., and Aswad, D. W. (2001) *Biochemistry 40*, 5747−5756.
21. Chevillard-Briet, M., Trouche, D., and Vandel, L. (2002) *EMBO J. 21*, 5457−5466.
22. Li, H., Park, S., Kilburn, B., Jelinek, M. A., Henschen-Edman, A., Asward, D. W., Stallcup, M. R., and Laird-Offringa, I. A. (2002) *J. Biol. Chem. 277*, 44623−44630.
23. Mestas, S. P., and Lumb, K. J. (1999) *Nature Struct. Biol. 6*, 613−614.
24. Campbell, K. M., and Lumb, K. J. (2002) *Biochemistry 41*, 13956−13964.
25. Edelhoch, H. (1967) *Biochemistry 6*, 1948−1954.
26. Cantor, C. R., and Schimmel, P. R. (1980) *Biophysical Chemistry*, Freeman, New York.
27. Pace, C. N. (1986) *Methods Enzymol. 131*, 266−280.
28. Santoro, M. M., and Bolen, D. W. (1988) *Biochemistry 27*, 8063−8068.
29. Pace, C. N., Shirley, B. A., and Thomson, J. A. (1989) in *Protein Structure* (Creighton, T. E., Ed.), IRL press, Oxford.
30. Laue, T. M., Shah, B. D., Ridgeway, T. M., and Pelletier, S. L. (1992) in *Analytical Ultracentrifugation in Biochemistry and Polymer Science* (Horton, J. C., Ed.) pp 90−125, The Royal Society of Chemistry, Cambridge.
31. Stryer, L. (1965) *J. Mol. Biol. 13*, 482−495.
32. Goto, Y., and Fink, A. L. (1989) *Biochemistry 28*, 945−952.
33. Semisotnov, G. V., Rodionova, N. A., Razgulyaev, O. I., Uversky, V. N., Gripas, A. F., and Gilmanshin, R. I. (1991) *Biopolymers 31*, 119−128.
34. Handel, T. M., Williams, S. A., and DeGrado, W. F. (1993) *Science 261*, 879−885.
35. Kuwajima, K. (1989) *Proteins 6*, 87−103.
36. Waldburger, C. D., Schildbach, J. F., and Sauer, R. T. (1995) *Nature Struct. Biol. 2*, 122−128.
37. Maxwell, K. L., and Davidson, A. R. (1998) *Biochemistry 37*, 16172−16182.
38. Camarero, J. A., Fushman, D., Sato, S., Giriat, I., Cowburn, D., Raleigh, D. P., and Muir, T. W. (2001) *J. Mol. Biol. 308*, 1045−1062.
39. Richardson, J. S., Richardson, D. C., Tweedy, N. B., Gernet, K. M., Quinn, T. P., Hecht, M. H., Erickson, B. W., Yan, Y., McClain, R. D., Donlan, M. E., and Surles, M. C. (1992) *Biophys. J. 63*, 1186−1209.
40. Betz, S. F., Raleigh, D. P., and DeGrado, W. F. (1993) *Curr. Opin. Struct. Biol. 3*, 601−610.
41. Gary, J. D., and Clarke, S. (1998) *Prog. Nuc. Acid Res. Mol. Biol. 61*, 65−131.
42. McBride, A. E., and Silver, P. A. (2001) *Cell 106*, 5−8.

BI0343976